Modeling of an Optimized Electrostimulative Hip Revision System Under Consideration of Uncertainty in the Conductivity of Bone Tissue

Christian Schmidt, *Member, IEEE*, Ulf Zimmermann, and Ursula van Rienen, *Member, IEEE*

***Abstract*—Since several years, the number of total hip arthroplasty revision surgeries is substantially growing. One of the main reasons for this procedure to become necessary is the loosening or damage of the prothesis, which is facilitated by bone necrosis at the implant–bone interface. Electrostimulation is one promising technique, which can accelerate the growth of bone cells and, therefore, enhance the anchorage of the implant to the bone. We present computational models of an electrostimulative total hip revision system to enhance bone regeneration. In this study, the influence of uncertainty in the conductivity of bone tissue on the electric field strength and the beneficial stimulation volume for an optimized electrode geometry and arrangement is investigated. The generalized polynomial chaos technique is used to quantify the uncertainty in the stimulation volumes with respect to the uncertain conductivity of cancellous bone, bone marrow, and bone substitute, which is used to fill defective areas. The results suggest that the overall beneficial stimulation areas are only slightly sensitive to the uncertainty in conductivity of bone tissue. However, in the proximity of tissue boundaries, larger uncertainties, especially in the transition between beneficial and understimulation areas, can be expected.**

***Index Terms*—Electrical stimulation, finite-element method, multiobjective optimization, total hip arthroplasty (THA) revision, uncertainty quantification.**

I. Introduction

HIP revision surgery, or more specifically a total hip arthroplasty (THA) revision, becomes necessary, if a previously implanted artificial hip joint or prothesis has to be replaced mainly due to a loosening or damage of the prothesis and to restore the patient's mobility. Since the 1990s, the number of such THA revision surgeries increased constantly and is predicted to grow substantially in the next decades by more than 130% [1]. In addition, about one-third of these THA revisions have to be revised. The demand to again revise the hip revision is mainly due to aseptic implant loosening, which is a result of mechanical instability at the implant–bone interface [2]. Besides the influence of mechanical stress, the aseptic implant loosening is facilitated by bone necrosis occurring at the implant–bone interface. Therefore, the reduction of the death of bone cells at this interface is one key aspect to increase the durability of these implants. One possibility to reduce the bone necrosis is to enhance the regeneration of the bone by facilitating the growth of bone cells at the implant–bone interface. In 1974, Basset *et al.* [3] showed that electrostimulation of bone cells had an accelerating effect on their growth and, therefore, can be applied in the healing process of fractures and bone defects. Until today, several high- and low-frequency stimulation systems, which are based on this effect, have been developed to provide an improved regeneration of the bone [4], [5].

A prototype of such an electrostimulative hip revision system is currently developed by the Orthopedic Institute at the University Medicine of Rostock. The prototype consists of an inductively coupled system to induce an electric field distribution of a certain intensity in an area around the implant, which is considered to be beneficial for bone growth and bone recovery. To provide the optimal positioning of the stimulation electrodes, a computational model of the hip revision system, comprising the implant as well as a model of a pelvic bone, was developed and subjected to a multiobjective optimization algorithm [6]. This optimal positioning of the stimulation electrodes is based on the model parameters comprising the geometry of the implant and the pelvic bone as well as the electric conductivity of the bone, which influences the resulting electric field pattern and, therefore, the extent of the area, which is beneficial to the growth of bone cells. While the geometry parameters are fixed and controllable in the considered hip revision system [7], the electric conductivity of bone tissue is subject to uncertainty in the literature [8], [9]. In addition, an artificial material, which is designed to substitute the mechanical and electrical properties of bone tissue, is used to fixate the implant and to fill gaps between the implant and the bone. Since this material often comprises disintegrated parts of cancellous bone, its electrical properties depend on that of the bone tissue and its composition. This uncertainty in the electrical properties of bone tissue and bone substitute results from the heterogeneity and composition of the materials, as well as from deviations in the measurements of biological tissue, *in vivo* and *ex vivo* [10]. In order to investigate the influence of these parametric uncertainties on the optimized stimulation protocol of the implant, it is necessary to quantify the uncertainty in the resulting electric field distribution and the optimal stimulation area.

This study aims at the uncertainty quantification of the electric field and the stimulation area in an electrostimulative hip revision system with respect to uncertainty in the electric conductivity of bone tissue and bone substitute. To reduce the

Manuscript received December 8, 2014; revised March 12, 2015; accepted April 10, 2015. Date of publication April 17, 2015; date of current version July 23, 2015. This work was supported by the German Science Foundation Research Training Group 1505 "Welisa."

The authors are with the Institute of General Electrical Engineering, University of Rostock, 18059 Rostock, Germany (e-mail: christian.schmidt6@uni-rostock.de; ulf.zimmermann@uni-rostock.de; ursula.van-rienen@uni-rostock.de).

Color versions of one or more of the figures in this paper are available online at http://ieeexplore.ieee.org.

Digital Object Identifier 10.1109/JBHI.2015.2423705

2168-2194 © 2015 IEEE. Translations and content mining are permitted for academic research only. Personal use is also permitted, but republication/redistribution requires IEEE permission. See http://www.ieee.org/publications_standards/publications/rights/index.html for more information.

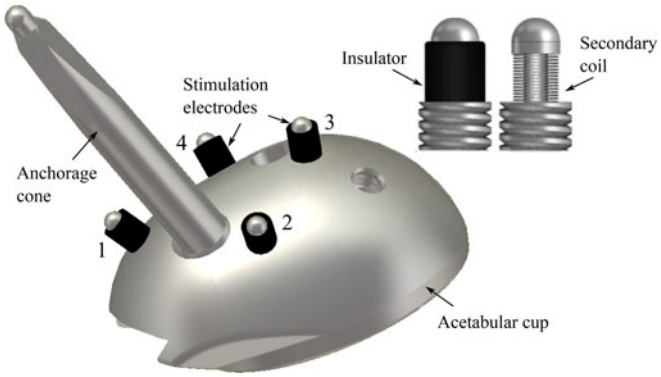

Fig. 1. Model of the acetabular cup including anchorage cone and four stimulation electrodes.

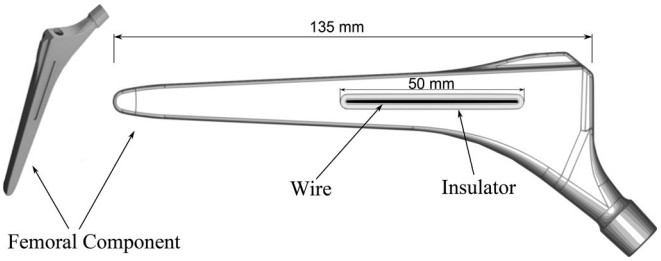

Fig. 2. Model of the femoral component including the stimulation electrode and insulator.

computational expense for the quantification of this uncertainty in the model solution, the generalized polynomial chaos (gPC) technique is used, which determines a simply evaluable surrogate model of these quantities of interest. This method is nonintrusive, which means that no change to the implementation of the deterministic model is required, and was already successfully applied in previous studies regarding bioelectrical applications [11], [12]. A preliminary version of this study has been reported in [13].

II. Methods

A. Electrostimulative Hip Revision System

The electrostimulative hip revision system contains an acetabular and a femoral component. The acetabular component has stimulation electrodes attached to its surface, which are connected via a coil inside an insulation layer (see Fig. 1). The hemispherical stimulation electrodes have a diameter of 4 mm, while the ovoid cup has a length of 70 mm and a width of 58 mm. The acetabular cup also includes an anchorage cone, which is placed in one of five default drill holes within the cup. The femoral component used in this study is a preliminary prototype still in its design state. So far, the component is composed out of a hip stem (Hipstar, size 2)[1] with a notch on one side of the implant, in which the stimulation electrode (width: 1.45 mm) and the surrounding biocompatible insulator are located (see Fig. 2).

A primary coil, which is placed around the patient's hip, provides a time-harmonic magnetic field at a frequency of 20 Hz. This oscillating field induces a location-dependent current in the secondary coils of the stimulation electrodes of the acetabular cup and the femoral component resulting in an electric potential distribution in the area around the implants. During surgery, each electrode of the acetabular cup has to be placed into the bone, which limits the number of utilizable stimulation electrodes. In this study, we use four electrodes for the acetabular cup. The model of the femoral part in its preliminary version consists of one fixated electrode, which has been tested in a porcine femur.

In this study, the acetabular component of the implant is attached to the pelvic bone of a human patient. The pelvic bone is represented as a layered computer-aided design (CAD) model, which is derived from computer tomography (CT) scans of a healthy pelvic bone. Due to the damage of the primary implant, the bone generally shows defects in the femoral and acetabular areas, which comprise cavities as well as discontinuities. To emulate this defective state, a cavity is manually inserted into the CAD model of the pelvic bone, which resembles the geometry of the former implant and the area of damaged tissue due to bone necrosis.

The design of the prototype of the electrostimulative hip stem used in this study is based on results from experimental studies carried out for a porcine femur. Therefore, the computational model of the hip stem is inserted into the CT-based CAD model of such a porcine femur. Due to the adolescence of the porcine test subject, the medullary cavity is larger than in adult human femoral bones. For this reason, the conductivity of bone marrow inside this cavity is also considered in the modeling of the femoral component. The stimulation electrode is connected to a secondary coil, which geometry and location within the final femoral component will be chosen to provide the required stimulation amplitude for beneficial stimulation of the bone determined in the computational model.

B. Computation of the Electric Field Distribution

The computation of the generated electric field distribution in the pelvic and femoral bone, which results from the induced oscillating field in the stimulation electrodes of the acetabular cup and the femoral component, is carried out by using the software CST EM Studio[2]. The acetabular cup is attached to the pelvic bone, which has been altered to show a central cavity to emulate a type 2C defect, as defined by Paprosky and Magnus [14]. The cavity is replenished with bone substitute to provide an adjoining interface between the implant and the bone (see Fig. 3). Since the prototype of the femoral component is investigated with regard to a porcine femur, in which the medullary cavity is larger than in adult human femoral bones, we focused on the investigation of the influence of uncertainty in the conductivity of bone marrow and cancellous bone for the femoral component.

The electric potential $\varphi(\boldsymbol{r})$ in the bone tissue and at the surface of the implant is computed by solving the Laplace's equation

[1]http://bizwan.com/_mydoc/stryker/Hip/HipStar TMZF Cementless Hip System Surgical Technique.pdf.

[2]CST Studio Suite 2012, http://www.cst.com/.

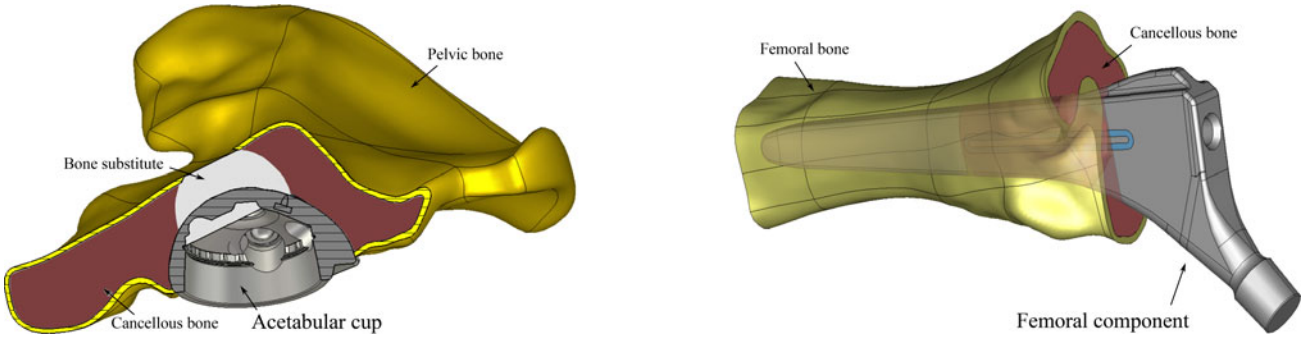

Fig. 3. Left: Acetabular cup fixated in the model of the pelvic bone with the defect filled up with bone substitute. Right: Femoral component fixated in the model of the porcine femoral bone.

within the computational domain Ω

$$\nabla \cdot [\sigma(\boldsymbol{r}) \nabla \varphi(\boldsymbol{r})] = 0, \quad \boldsymbol{r} \in \Omega \tag{1}$$

which represents a volume conductor with purely resistive tissue and material properties described by their electric conductivity $\sigma(\boldsymbol{r})$. The consideration of solely the conductivity of bone tissue is possible, because due to the low frequency of 20 Hz, the strength of the displacement currents and eddy currents in the model is negligibly small compared to the strength of the conductive currents within the tissues [6]. The (1) is discretized at the nodes of the model mesh using the finite-integration technique [15], which is implemented in CST EM Studio. Depending on the alignment of the secondary coil in the magnetic field, the electric potential of each stimulation electrode is determined based on the approach of Potratz *et al.* [6]. The potential at the electrode surface in the discretized model is described by inhomogeneous Dirichlet boundary conditions, while the remaining surface of the implant components Ω_{surf} is set to a reference potential of $\varphi(\boldsymbol{r}) = 0\mathrm{V}$, $\boldsymbol{r} \in \Omega_{\mathrm{surf}}$. Both models are discretized in a hexahedral mesh, using local mesh refinement in the area of interest and applying an automated adaptive refinement. For this purpose, the models were imbedded into a cuboid-shaped insulator. For the femoral part, a manual convergence study has been carried out by using the power loss as a reference value. The final meshes consisted out of approximately 10.1 million hexahedral elements for the acetabular simulation model and approximately 1.6 million hexahedral elements for the femoral simulation model. The solution was computed by using the stationary currents solver of CST EM Studio with a solver accuracy of 1×10^{-9}.

C. Optimization of the Electrode Arrangement

The accelerating effect on the growth of bone cells by electrostimulation described by Basset *et al.* [3] depends on the electric field distribution in the bone. This field distribution is determined by the placement of the stimulation electrodes on the implant and depends also on the geometry of the pelvic bone as well as the femoral part and the individual defects as classified in [14]. While the femoral component of the implant has a fixed stimulation electrode located in a notch of the implant (see Fig. 2), the stimulation electrodes on the acetabular cup can be placed at different locations to provide a preferably large beneficial stimulation region. To provide the optimal electrode arrangement for the acetabular cup, we apply a multiobjective evolutionary optimization algorithm as presented in [6]. Based on the work of Kraus [16] and clinical advice, an electric field of 5–$70\,\mathrm{V/m}$ in the proximity of the implant and 35–$70\,\mathrm{V/m}$ in the defective area, which both forms the area of interest, is considered to be optimal. These requirements constitute the primary and secondary optimization goals for the acetabular component, respectively. Accordingly, an electric field above these threshold values is considered to facilitate bone damage due to the death of bone cells caused by overstimulation and an electric field below these threshold values to have no beneficial effect on the growth of bone cells [16]. The stricter definition for the second goal is due to the emphasis on the stimulation of the defective area. Here, a complete bone remodeling process has to take place, while the healthy bone is stimulated to regenerate after the surgery and to attach well to the implant. Due to the limited number of stimulation electrodes to cover the whole implant surface, high stimulation amplitudes, resulting in high potentials in the proximity of stimulation electrodes, are required to provide the minimal threshold values for beneficial stimulation in the area of interest. On the contrary, these high potentials at the stimulation electrodes cause large areas of overstimulation. Therefore, the optimization process requires a tradeoff between avoiding overstimulation and facilitating a beneficial electric field strength in the area of interest. For this reason, a multiobjective genetic optimization algorithm is applied.

For the multiobjective optimization, the nondominated sorting genetic algorithm-II is applied [17]. For an initial population, which comprises a set of 200 random arrangements of the four electrodes, the algorithm computes the electric field distribution for all arrangements and evaluates them with respect to the optimization goals, described earlier in this section. From this set, the best arrangements are used in the next generation of the population. This is repeated until one of the following conditions is reached. The first condition is that every point in the area of interest shows the desired electric field. The second condition is that multiple consecutive generations show the same electrode arrangement, which is a sign for the convergence of the solution to a stable state. The third breaking condition is fulfilled when the maximum of 200 iterations is reached. The final solution is shown as a set of Pareto optimal arrangements,

from which one can be chosen manually or automatically [7]. This decision can be based on further parameters, like the applicability of the arrangements during surgery, or on a subsequent preference of one stimulation goal within this Pareto optimal set of arrangements. Since for every arrangement, the fulfillment of each optimization goal is represented by a scalar value, the optimal arrangement was selected by minimizing both goal functions equally in this study.

Due to the linearity of the electrical properties of bone tissue with respect to the electric field at a fixed frequency [6], the principle of superposition can be applied to determine the electric field distribution of each possible electrode arrangement by a linear combination of the electric field distributions generated by each single electrode. The required basic field distributions are computed with the finite-integration technique using CST EM Studio by subsequently applying a stimulation amplitude of 1 V at one electrode at each point of an equidistant (1.5 mm) grid with 4489 possible electrode positions across the surface of the acetabular cup. The electric field in the whole area of interest is interpolated from the determined solution at these points. This approach allows for separating the computational expensive simulation of the discretized model from the optimization process and, therefore, enables the optimization process to be carried out in the postprocessing, which substantially reduces its computational expense.

For the optimization of the electrode geometry of the femoral component, the design parameters are comprised by the width of the electrode and its surrounding insulator as well as the applied stimulation amplitude. To sustain mechanical stability, the notch inside the hip stem and, therefore, the surface of the insulator, has to be kept as small as possible. Contrary, an increase in the insulator area would also increase the extent of the beneficial stimulation volume. These goals constitute a similar tradeoff condition as for the acetabular component. Since the femoral component used in this study comprises a prototype investigated in a porcine femur, the focus is on the influence of uncertainty in the conductivity of bone tissue. For this reason, only the first optimization goal, to provide an electric field strength between $5 - 70$ V/m in the area of interest, is used for the femoral component. The optimization is carried out with the trust region framework [18] implemented in CST EM Studio. This iterative optimization method compares mutually different realizations of the model to choose the superior realization based on the performance of the considered goal functions within a trust region. This trust region is a subsection of the area of interest. If the new local model fulfills the goal functions within this subsection, the trust region is increased for the next model realization. If the goal functions are not fulfilled, the trust region is decreased. The optimization process stops either when all goal functions are reached within the whole area of interest, or when the radius of the trust region becomes smaller than the specified domain accuracy.

D. Modeling of the Bone and Bone Substitute Conductivity

The measurement of the electrical properties of biological tissue constitutes a challenging task associated with difficulties in the measuring process regarding the proper consideration of several effects, such as electrode polarization at low frequencies and changes in the conditions of the tissue samples. Due to ethical concerns and practical reasons, measurements are often performed *ex vivo* on excised tissue samples, which can lead to changes of the electrical properties of biological tissue [19]. As a result, different values for the conductivity of bone tissue can be found in the literature [8], [9]. In addition, bone substitute is an artificial material, whose composition comprises parts of disintegrated cancellous bone. Therefore, its electrical properties depend not only on those of cancellous bone, but also substantially on its composition. To account for this variability in the electrical properties of cancellous bone and bone substitute, their conductivity values are modeled to be uniformly distributed random variables in $\mathcal{U}[a, b]$, where the lower and upper boundaries are based on the values found in the literature (see Table I). The use of uniform distributions accounts for the lack of data and assumes each conductivity within the set boundaries to be of the same probability, which resembles a kind of a "worst-case" scenario. Due to the possibly large variability in the fabrication process of bone substitute, its conductivity is modeled for different levels of uncertainty, determined by its respective relative deviation, which is defined by the distance of the upper and lower boundary divided by the respective mean value. Since the cortical bone compartment surrounds the major compartment comprised of cancellous bone, and, therefore, has a minor influence on the electric field strength in the proximity of the surfaces of the implants, its conductivity was modeled deterministic and set to a value of 20 mS /m [8].

TABLE I
LOWER AND UPPER BOUNDARY, AND RELATIVE DEVIATION OF THE UNIFORMLY DISTRIBUTED CONDUCTIVITIES OF CANCELLOUS BONE, BONE MARROW, AND BONE SUBSTITUTE

Tissue type	**Conductivity** σ $[\mathrm{mS/m}]$		
	Min	**Max**	**Rel. Deviation**
Cancellous bone	78.9	150	31.1%
Bone marrow	1.3	101	97.5%
Bone substitute (5%)	105	124	8.66%
Bone substitute (10%)	94.6	134	17.3%
Bone substitute (20%)	74.8	154	34.6%
Bone substitute (40%)	35.2	194	69.3%

Bone substitute was modeled for different relative standard deviations with respect to a mean conductivity of 114 mS/m.

E. Uncertainty Quantification Using Polynomial Chaos

The beneficial stimulation region resulting from the previously computed optimal electrode arrangement of the acetabular cup determined by the multiobjective evolutionary algorithm and from the stimulation of the femoral component depend on the conductivity of bone tissue and bone substitute. The uncertainty in these model parameters result in an uncertainty in the determined electric field and, therefore, in the predicted beneficial stimulation region. To investigate the influence of the uncertainty in the model parameters on the model solution, stochastic

methods such as Monte–Carlo simulation (MCS) are required. Such probability sampling methods determine the statistics of the model solutions of interest by computing random realizations of the deterministic model based on random samples of the uncertain model parameters. In general, such methods require a large number of model realizations to provide a sufficient accuracy in the statistics of the model solutions [20]. Since the computation of the deterministic model requires a considerable amount of computational resources and time, as noted in Section II-C, the application of MCS for the quantification of the uncertainty in the model solutions is not practical. To reduce the number of required model realizations, the gPC technique is applied, which determines a simply evaluable surrogate model by using the deterministic model as some kind of a "black-box" [20]. This "nonintrusive" property of the method does not require changes to the code, which describes the deterministic model. Since the model is generated by using commercial software to determine the beneficial stimulation region, this property comprises a crucial factor in the uncertainty quantification of its solutions.

The main idea of the gPC technique is to determine a surrogate model of the model solution or derived quantity of interest $Y(\omega)$, with ω indicating its statistical properties, by expanding the model solution in a series of multivariate orthogonal basis functions $\psi\left(\boldsymbol{\xi}(\omega)\right)$, depending on the random vector $\boldsymbol{\xi}(\omega) = (\xi_1(\omega), \ldots, \xi_M(\omega))$ with $\xi_i(\omega) \in \mathcal{U}[-1, 1]$, for which the optimal choice of basis functions is determined by the product of univariate Legendre polynomials [21]. In general, this series expansion is truncated at a certain expansion order p, which determines the number P of basis functions [20]. The corresponding coefficients $c_k, k = 1, \ldots, P$ are determined by projecting the basis function $\psi_k\left(\boldsymbol{\xi}(\omega)\right)$ onto the model solution $Y(\omega)$. Since the probability distribution of the solution is unknown, the integral formulation resulting from the projection has to be computed by numerical integration, for which the model solution Y(ω) and, therefore, the deterministic model is evaluated at the prescribed integration nodes selected from the model parameters $\boldsymbol{X}(\omega) = (X_1(\omega), \ldots, X_M(\omega))$. Since the random parameters $X_i(\omega)$ are uniformly distributed, the mapping on the corresponding random variables $\xi_i(\omega)$, which is required for the series expansion in the basis functions $\psi\left(\boldsymbol{\xi}(\omega)\right)$, can be carried out by a linear transformation [11]. In general, the generation of integration nodes, which comprise the deterministic samples of the model parameters, are based on a tensor-grid approach. These tensor grids comprise all combinations of the integration nodes for each model parameter, which results in an exponential growth of the number of integration nodes with the number of model parameters M. To partly overcome this so-called "curse of dimensionality," sparse-grid methods can be applied, which reduce the number of integration nodes compared to tensor grids by attributing less weight on the basis functions with mixed higher order polynomials [22]. In a preliminary version of this study, tensor grids were used to compute the coefficients of the gPC expansions for the beneficial stimulation region of the acetabular cup [13]. The results of this investigation suggested that the model solution was not dependent on mixed higher order polynomials in the gPC expansions. Therefore, the computationally more efficient sparse grid methods based on the approach described by Constantine *et al.* [22] are used in this study.

F. Determining the Uncertainty in the Stimulation Regions

To provide a measure on how the uncertainty in the conductivity of bone tissue influences the stimulation of bone tissue in the considered electrostimulative hip revision system, the regions of under-, beneficial, and overstimulation are computed for the acetabular component and the femoral component. These regions are determined by computing the uncertainty in the electric field norm for a set of sampling points located in the proximity of the implant–tissue interface and using a tetrahedral mesh to obtain the corresponding volumes. Although, the whole bone can benefit from a stimulation field above 5 V/m, the focus of this study is in the stimulation of the close proximity to the implants. For the acetabular component, the sampling points were positioned in 15 equidistant layers between 1- and 15-mm distance to the surface. Each layer comprises sampling points positioned over the whole surface within the bone using a step size of 1 mm. Adding up all layers, the total number of sampling points for the acetabular cup is $61\,184$. A similar sampling is used for the femoral component across the area of the stimulation electrode. Since the prototype of the femoral component comprises only one stimulation electrode, which is located in a notch of the implant, the electric field of the electrostimulative hip stem does not reach that deep into the bone as compared to the acetabular cup. Therefore, the sampling points are located in six layers between 0.5 and 5.5 mm normal to the surface, and a range of 13 and 47 mm with a step size of 0.5 and 1 mm in the x- and y-component of each layer, respectively, resulting in a total of 7776 sampling points. Due to the different sizes of the areas of interest, the optimization of the beneficial stimulation volumes resulted in different stimulation amplitudes at the electrodes in both models. For the acetabular cup, the determined stimulation amplitudes are 1.704, 1.699, 1.451, and 1.534 V at electrode 1 to 4 (see Fig. 1) and 0.17 V for the femoral component. The optimization of the electrode arrangement, geometry, and stimulation amplitudes was carried out for minimum conductivity of cancellous bone, while the conductivity of bone substitute and bone marrow was set to its mean and maximum value, respectively.

III. Results

The uncertainty quantification of the stimulation regions was carried out for the optimized hip revision system. The optimal electrode arrangement for the acetabular cup used in this study is based on preliminary work [13]. The optimization of the femoral component resulted in an optimal electrode and insulator width of 1.45 and 1.4 mm. For each sampling point $\boldsymbol{r}^{(k)}, k = 1, \ldots, N_\mathrm{s}$ in the models, the gPC expansion of the electric field strength $E\left(\boldsymbol{r}^{(1)}\right)$ was computed, resulting in the electric field strength $\boldsymbol{E}_\mathrm{s} = \left(E\left(\boldsymbol{r}^{(1)}\right), \ldots, E\left(\boldsymbol{r}^{(N_\mathrm{s})}\right)\right)$ in the area of interest. To provide a measure for the approximation error estimation ϵ_{gPC} of the gPC expansions of the electric field strength, the difference in its variance $\mathbb{V}$ with respect to the applied expansion order p was evaluated *a posteriori* by

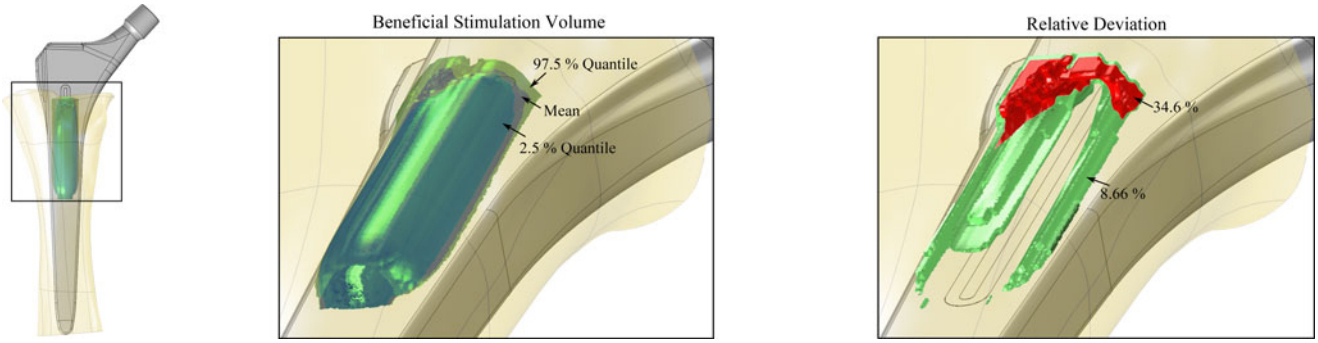

Fig. 4. Lower quantile (2.5%), upper quantile (97.5%), and mean of the beneficial stimulated area between 5 and 70 V/m for the femoral component. Uncertainty areas are shown for relative deviations larger than 8.66% and 34.6%, respectively.

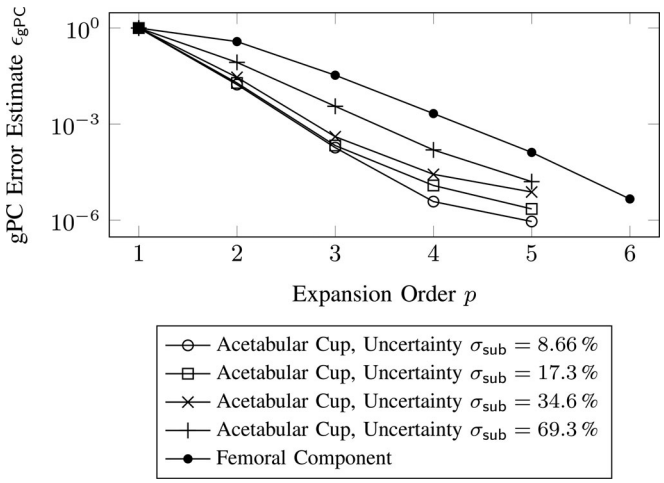

Fig. 5. Posteriori approximation error estimate ϵ_{gPC} of the variance of the electric field strength at the sampling points in the areas of interest for the acetabular and femoral component, respectively. For the acetabular component, the uncertainty in the conductivity of bone substitute was modeled with values between 8.66% and 69.3%.

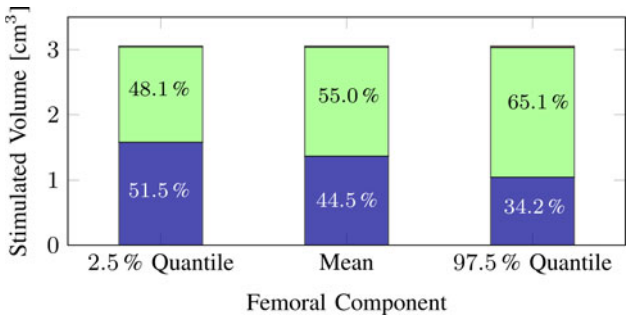

Fig. 6. Lower quantile (2.5%), upper quantile (97.5%), and mean of the over- (red), under- (blue), and beneficial (green) stimulated areas for the femoral component. The colors red, blue, and green are located at the top, bottom, and middle of the bars, respectively.

computing

$$\epsilon_{\mathrm{gPC}}(p) = \frac{\|\mathbb{V}\left[\boldsymbol{E}_{\mathrm{s}}\left(\boldsymbol{r}, p\right)\right] - \mathbb{V}\left[\boldsymbol{E}_{\mathrm{s}}\left(\boldsymbol{r}, p-1\right)\right]\|}{\|\mathbb{V}[\boldsymbol{E}_{\mathrm{s}}(\boldsymbol{r}, p)]\|}. \qquad (2)$$

A sufficient accuracy in the approximation error estimation of the gPC expansions for the considered sampling points was ensured by increasing the expansion order p until the estimate was below 1×10^{-4}, which required an expansion order of up to $p = 5$ for the acetabular component and $p = 6$ for the femoral component (see Fig. 5). These expansion orders resulted in a number of 145 and 321 required model realizations, respectively, to provide the model solution at the nodes of the corresponding sparse grids. Based on the determined gPC expansions for the electric field norm of the sampling points, their lower quantile, mean value, and upper quantile for a confidence interval of 95% were determined by applying MCS to the gPC expansions for a number of 10 000 random samples.

These stochastic measures of the electric field strength in the area of interest allowed for computing the corresponding stochastic measures for the volumes of under-, beneficial, and overstimulation. For the femoral component, the determined stimulation volumes resemble a cylinder-symmetrical shape around the stimulation electrode, except for the upper region close to the cutting plane (see Fig. 4). This upper region comprises several tissue boundaries between bone marrow, cancellous bone, and cortical bone, resulting in changes of the electric field strength in the proximity of these boundaries. As a consequence, the largest local deviations of the uncertain electric field strength can be found in this region with values in the range of the uncertainty modeled in the conductivity of cancellous bone and bone marrow. The beneficial stimulation volume includes nearly the complete anterior interface between implant and bone along with the electrode with a maximum stimulation depth for the mean beneficial stimulated area of 6 mm. Regarding the understimulated area, the beneficial stimulation volume deviates by approximately 15.7% regarding the lower quantile and by approximately 23.1% for the upper quantile compared to its mean value (see Fig. 6). In contrast, the overstimulated area shows only minor deviations in the lower and upper quantiles with respect to its mean value. The uncertainty in the beneficial stimulation volume is approximately 8.5% and, therefore, around one-fourth of the uncertainty modeled in the conductivity of cancellous bone and approximately 11 times smaller than that of bone marrow.

For the optimized four-electrode arrangement of the acetabular cup, the uncertain beneficial stimulation volume regarding the second optimization goal with an electric field strength between 35 and 70 V /m is shown in Fig. 7 . For this study case,

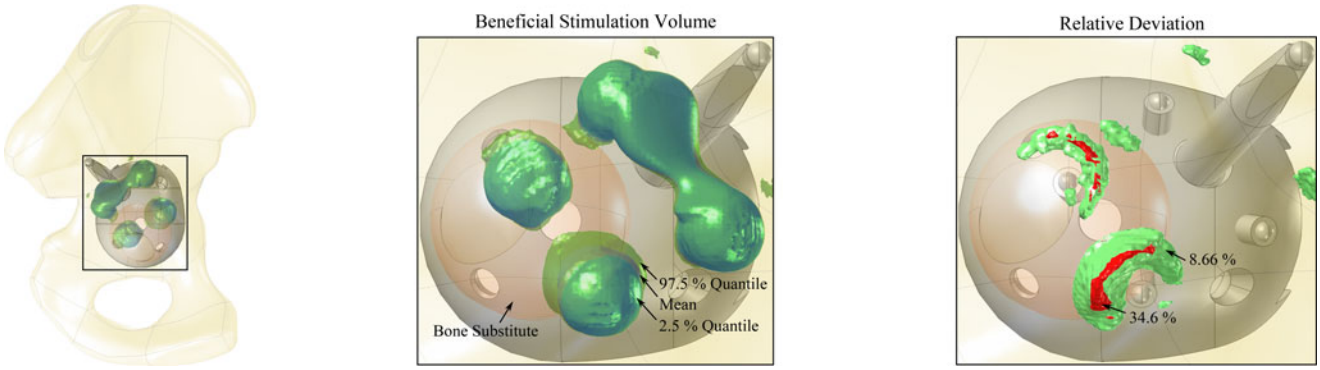

Fig. 7. Lower quantile (2.5%), upper quantile (97.5%), and mean of the beneficial stimulated area between 35 and 70 V/m for the acetabular component with an uncertainty in the conductivity of bone substitute of 69.3%. Uncertainty areas are shown for relative deviations larger than 8.66% and 34.6%, respectively.

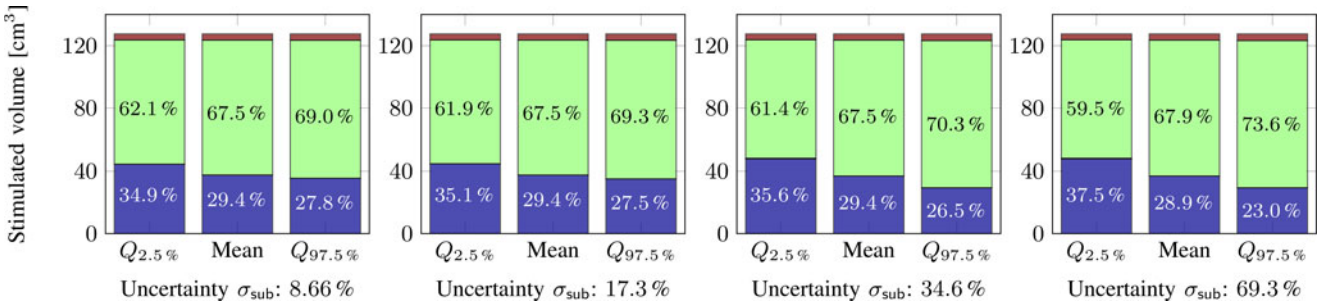

Fig. 8. Lower quantile (2.5%), upper quantile (97.5%), and mean of the over- (red), under- (blue), and beneficial (green) stimulated areas for the acetabular cup shown for different levels of uncertainty in the conductivity of bone substitute. The colors red, blue, and green are located at the top, bottom, and middle of the bars, respectively.

the level of uncertainty in the conductivity of bone substitute was set to 69.3%. One electrode is located nearly in the center inside of the defective area, and another one close to the tissue boundary between bone substitute and cancellous bone, while the remaining electrodes are located closer to the anchorage cone inside the cancellous bone compartment. The beneficial stimulation volumes for the second optimization goal resemble an almost spherical shape, except for the electrode close to the anchorage cone. The quantiles of this beneficial stimulation volume deviate at most at the tissue boundary between the defective area, filled with bone substitute, and the cancellous bone compartment. The beneficial stimulation areas with an uncertainty larger than 8.66% are comparatively small regarding the whole beneficial stimulation volume and are as well small in magnitude compared to the uncertainty in the conductivity of bone substitute (69.3%) and cancellous bone (31.1%). Smaller areas of beneficial stimulation for the upper quantile are noticeable behind the anchorage cone. Due to application of an optimized four-electrode system, the beneficial stimulation volume covers a large area of the pelvic bone. Since the focus of this study is on the investigation of the beneficial stimulation in the proximity of the implant, only that volumes for the second optimization goal (35–70 V/m) were illustrated. To investigate the extent of the uncertain beneficial stimulation volumes regarding the first optimization goal, their size within the area of interest was compared to the volumes of under- and overstimulation for an uncertain conductivity in bone substitute from 8.66% up to 69.3% (see Fig. 8). While the mean value of the beneficial stimulation volume was similar for all cases, the uncertainty increased from approximately 5% to 10.4%. The uncertainty in the overstimulation volume was comparatively small with values ranging from approximately 2% to 6%. Compared to the size of the beneficial stimulation volume, the absolute deviation in the overstimulation volume was negligible. Therefore, the uncertainty in the beneficial stimulation volume resulted in mainly a corresponding uncertainty in the understimulation volume.

The mean value of the beneficial stimulation volume for different levels of uncertainty in bone substitute conductivity did not change substantially, while the uncertainty in the volume increased continuously with a larger increase with respect to the lower quantile compared to the upper quantile (see Fig. 9). The increase of the lower and upper quantile was nonlinear, being in good agreement with a quadratic fitting function. Compared to the levels of uncertainty in bone substitute conductivity, the uncertainty in the beneficial stimulation volume was substantially smaller. The ratio between the uncertainty in the beneficial stimulation volume and bone substitute increased from a factor 1.7 for an uncertain conductivity of 8.66% up to a factor of 6.7 for an uncertain conductivity of 69.3%.

IV. Discussion

The objective of this study was to investigate the influence of uncertainty in bone tissue conductivity on the beneficial stimulation of bone cells in the proximity of the surface of an electrostimulative hip revision system. Computational models

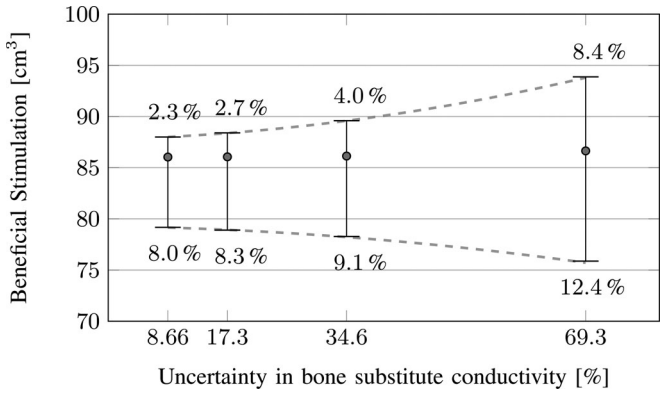

Fig. 9. Lower quantile, upper quantile, and mean of the beneficial stimulation volume for the acetabular cup shown for different levels of uncertainty in the conductivity of bone substitute.

of an acetabular component and femoral component of a prototype system were attached to realistic 3-D models of the pelvic and femoral bone. Electrode arrangements and geometry were optimized in order to provide an optimal beneficial stimulation in the proximity of the surface of the implants. Based on the method of Kraus, beneficial stimulation was assumed in regions, where the electric field strength was between 5 and 70 V/m at a frequency of 20 Hz [16]. The goal of Kraus' method is to achieve a beneficial cellular response in a large region in the proximity of the implant surface. *In vitro* experiments demonstrated that alternative low-frequency electrostimulative methods as well as dc-polarization approaches may also facilitate a beneficial cellular response by promoting osteoblast functions like proliferation and calcification at the surface of conducting implant materials, but with comparably lower electric field strengths [23], [24]. The optimal thresholds for the electric field strength to provide beneficial stimulation are still subject of ongoing research [25]. For the acetabular cup, the second goal to provide an electric field between 35 and 70 V/m within the defective region has been introduced. This stricter optimization goal and the larger beneficial stimulation region of the acetabular cup compared to the region of the femoral part facilitate higher stimulation amplitudes for the acetabular cup, which resulted in different stimulation amplitudes of both implant parts.

The uncertainty in the electric field strength in the areas of interest with respect to the uncertainty in the conductivity of bone tissue and bone substitute was determined by using the gPC technique. The gPC expansions of the electric field strength in the areas of interest for the acetabular component and femoral component were computed for expansion orders up to $p = 5$ and $p = 6$, which required the computation of the deterministic model for 145 and 321 different sets of conductivity values. MCS with $10\,000$ random samples of the uncertain bone tissue conductivities was applied to the determined gPC expansions to compute the stochastic measures of the electric field strength for each point of interest. This number of random samples was required to reduce the error estimate of the variance in the electric field strength to below 1%. Due to the large number of sampling points in the areas of interest, the number of random samples was chosen to provide a reasonable accuracy in the stochastic measures, while allowing for their computation in a reasonable time on common workstations. The computation time of the model solution of the acetabular component and the femoral component for the 145 and 321 model realizations, which were required to provide gPC expansions of the order $p = 5$ and $p = 6$, was approximately 43.5 and 16 h, respectively (workstation with 4×3.6 GHz, 64-GB RAM). The computation time of the gPC expansions and the application of MCS on the expansions for all sampling points in the areas of interest was approximately 10.3 and 2.7 h, respectively. Therefore, the whole computation time for the uncertainty quantification in the stimulated areas was approximately 54 h for the acetabular component and 19 h for the femoral component. In comparison, the application of MCS directly to the models for the same number of $10\,000$ random samples would have required a computation time of approximately four month for the acetabular component and 21 d for the femoral component, using the same workstation without considering additional computational resources, and would only allow for an accuracy in the variance of the electric field strength in the considered models of approximately 1%. Therefore, the applied gPC method in combination with the sparse integration approach [22] allowed for a substantial reduction of the computational expense and required computational resources in this study.

The quantiles and mean value of the electric field strength for a confidence interval of 95% in the area of interest were used to determine the volumes of under-, over- and beneficial stimulation. For the femoral component, almost the entire lateral interface between the implant and the femoral bone is beneficially stimulated and resembles a cylindrical shape (see Fig. 4). This shape results from the homogeneous conductivity in the area of interest, dominated by the cancellous bone compartment. Evidence for this behaviour can be derived from (1). In the case, that a compartment boundary is sufficiently far away from the stimulation electrode, the electric field distribution approaches that for the homogenous Laplace equation, resulting in nullification of the influence of uncertainty in the conductivity of the corresponding bone tissue. Therefore, the electric field strength close to the stimulation electrodes is hardly affected by the uncertainty in bone tissue conductivity, which explains the minor deviations in the overstimulation volumes. However, in the upper part of the bone deviations from this shape can be found, which result from conductivity changes across the boundaries between the bone tissue compartments (Compare Fig. 3, right). In this area, the bone marrow is comparatively small with regard to cancellous bone, and the overall shape of the bone deviates from the more cylindrical shape in its lower part, resulting in two compartment boundaries in close proximity to the stimulation electrodes, which are the reason for these deviations. Regarding the uncertainty of the electric field strength in this area, the largest deviations are located in the proximity of the bone tissue boundaries. However, the overall uncertainty in the beneficial stimulation volume is approximately 8.5% and, therefore, only around one-fourth of the uncertainty modeled in the conductivity of cancellous bone and approximately 11 times smaller than that of bone marrow (see Fig. 6). Taking into account a uniform distribution, the corresponding variance of the beneficial

stimulation volume is below 5%, which is considered as tolerable.

For the acetabular component, the largest deviations in the uncertain beneficial stimulation volumes with regard to the second optimization goal occur in the proximity between the boundary of bone substitute and cancellous bone, which is consistent with the results for the femoral component (see Fig. 7). In addition, the second optimization goal facilitates these deviations by enforcing a stricter condition on the electric field strength in the defective area. Therefore, the closer an electrode is located to these bone tissue boundaries, the larger the deviations in the uncertain beneficial stimulation volumes can be expected. Regarding the second optimization goal, the beneficial stimulation volumes resemble a spherical shape, except for the first and second electrode located close to the anchorage cone, which perturbates the shape of the volumes. In addition, smaller areas of beneficial stimulation for the upper quantile of the electric field strength are noticeable behind the anchorage cone, which result from the conductivity ratio between cancellous bone and cortical bone at their compartment boundary. However, the size of these areas and their level of uncertainty is comparatively small to the overall beneficial stimulation volume. Due to the comparatively large stimulation amplitudes determined for the optimized electrode arrangement of the acetabular cup to that of the femoral component, the beneficial stimulation volume with regard to the first optimization goal covers a larger portion of the sampled region and with that larger areas of overstimulation (see Fig. 8).

Similar to the results for the femoral component, the deviations in the uncertain overstimulation volumes are negligibly small compared to the uncertainty in the conductivity of the considered bone tissue types. This result is in agreement with the local deviation areas depicted in Fig. 7, which show the largest deviations at the transition between the uncertain beneficial- and understimulation volumes. Compared to the size of the beneficial stimulation volume of the acetabular cup (see Fig. 8) that of the femoral component is substantially smaller (see Fig. 6). Besides the larger stimulation amplitudes at the electrodes of the acetabular cup they are located at the surface and penetrate the bone. In contrast, the prototype of the femoral component has only one electrode, which is located in a notch in the implant. A larger insulator would allow for higher stimulation voltages at the electrode, which would lead to a larger beneficial stimulated area. However, this increase of the insulator size would result in a larger area, at which the bone can only poorly connect, which would contradict the optimization goals. Besides, the overstimulation volume for the femoral component is comparatively small. In the future design of the femoral implant, the option to use multiple stimulation electrodes is considered, which would also require an increase in the area of interest to cover a larger surface of the implant and, therefore, would also result in larger stimulation amplitudes and an increase in the insulator size to optimally stimulated the area.

For the acetabular cup, the uncertainty in the beneficial stimulation volume increased with increasing uncertainty in the conductivity of bone substitute, but was considerably smaller in magnitude with ratios from 1.7 for 8.66% uncertainty in bone substitute conductivity to 6.7 for 69.3% uncertainty (see Fig. 9). Compared to the level of uncertainty in bone substitute conductivity, the uncertainty in the beneficial stimulation volume increases by a substantially lower growth rate. To provide an uncertainty in the beneficial stimulation volume bounded by 8.66%, which is considered to be tolerably small, an uncertainty of up to 66% in bone substitute conductivity would be respectable. This large tolerance margin in the conductivity of bone substitute allows for the possible application of several substitute compositions and basic components. Furthermore, the results suggest that the influence of uncertainty in the conductivity of bone tissue and bone substitute on the beneficial stimulation volumes of the considered electrostimulative hip revision system is tolerably small. The optimized electrode arrangements and locations of the acetabular cup and geometry of the femoral component are quite insensitive to uncertainty in the conductivity of bone tissue as modeled in this study. However, it has to be kept in mind that in the proximity of tissue boundaries large local uncertainties can occur, which have to be controlled in the modeling and design process of such electrostimulative implants.

To the authors' knowledge, this study presents the first computational results and insights on how uncertainty in the conductivity of bone tissue influences the therapeutic effect of an electrostimulative hip revision system. The results of this study enhance the design and optimization process of the implants and allow for a prediction of the safety margins for their use. In future studies, the uncertainty quantification will be included in the optimization process to allow for a patient-individual optimization of the electrode arrangements under the consideration of minimal deviations in the beneficial stimulation volumes.

V. Conclusion

In this study, the influence of uncertainty in the conductivity of bone tissue for an optimized electrostimulative total hip revision system was investigated. For this purpose, the system, which consists out of a femoral and an acetabular component, is optimized using realistic bone models to provide maximal regions of beneficial stimulation, while minimizing regions of overstimulation. For both parts, optimization algorithms have been used to reach the specific goals for the different bone types. The optimized system was used to determine the influence of uncertainty in the conductivity of bone tissue on the beneficial stimulation areas for each model. The results suggest that the overall beneficial stimulation areas are only slightly sensitive with regard to uncertainty in the bone tissue conductivity. In particular, the overstimulated areas were found to be robust against the uncertainty in bone tissue conductivity. However, in the proximity of tissue boundaries, larger uncertainties, especially in the transition between beneficial and understimulation areas, can be expected.

Acknowledgment

The authors would like to thank the research team of R. Bader of the Orthopedic Institute at the University Medicine Rostock

for support and for providing the necessary CAD models of bones and implants.

REFERENCES

[1] S. Kurtz, K. Ong, E. Lau, F. Mowat, and M. Halpern, "Projections of primary and revision hip and knee arthroplasty in the United States from 2005 to 2030," *J. Bone Joint Surg. Amer.*, vol. 89, pp. 780–785, Apr. 2007.

[2] B. Springer, T. Fhering, W. Griffin, S. Odum, and J. Masonis, "Why revision total hip arthtroplasty fails," *Clin. Orthop. Relat. Res.*, vol. 467, pp. 166–173, Jan. 2009.

[3] C. Bassett, R. Pawluk, and A. Pilla, "Acceleration of fracture repair by electromagnetic fields. A surgically noninvasive method," *Ann. NY Acad. Sci.*, vol. 238, pp. 242–262, Oct. 1974.

[4] W. Latham and J. Lau, "Bone stimulation. A review of its use as an adjunct," *Techn. Orthop.*, vol. 26, pp. 14–21, Mar. 2011.

[5] R. Aaron, D. Ciombor, and B. Simon, "Treatment of nonunions with electric and electromagnetic fields," *Clin. Orthop. Relat. Res.*, vol. 419, pp. 21–29, Feb. 2004.

[6] C. Potratz, D. Kluess, H. Ewald, and U. van Rienen, "Multiobjective optimization of an electrostimulative acetabular revision system," *IEEE Trans Biomed. Eng.*, vol. 57, no. 2, pp. 460–468, Feb. 2010.

[7] U. Zimmermann and U. van Rienen, "An automatic Pareto classifier for the multiobjective optimization of an electrostimulative acetabular revision system," *IEEE Trans. Magn.*, vol. 50, no. 2, pp. 741–744, Feb. 2014.

[8] S. Gabriel, R. W. Lau, and C. Gabriel, "The dielectric properties of biological tissues: III. Parametric models for the dielectric spectrum of tissues," *Phys. Med. Biol.*, vol. 41, no. 11, pp. 2271–2293, Nov. 1996.

[9] H. Ewald, R. Bader, D. Kluess, R. Souffrant, C. Potratz, U. van Rienen, and W. Mittelmeier, "Untersuchungen der elektrischen und dielektrischen Eigenschaften von hüftknochen für den einsatz elektrostimulierender implanate," in *Proc. 5th Symp. Autom. Control*, 2008, pp. 1847–1850.

[10] C. Gabriel, A. Peyman, and E. H. Grant, "Electrical conductivity of tissue at frequencies below 1 MHz," *Phys. Med. Biol.*, vol. 54, pp. 4863–4878, Aug. 2009.

[11] C. Schmidt, P. Grant, M. Lowery, and U. van Rienen, "Influence of uncertainties in the material properties of brain tissue on the probabilistic volume of tissue activated," *IEEE Trans. Biomed. Eng.*, vol. 60, no. 5, pp. 1378–1387, May 2013.

[12] C. Schmidt and U. van Rienen, "Global sensitivity analysis of the probabilistic volume of tissue activated in a volume conductor model for deep brain stimulation," in *Proc. 6th Int. IEEE/EMBS Conf. Neural Eng.*, Nov. 2013, pp. 1218–1221.

[13] C. Schmidt, U. Zimmermann, and U. van Rienen, "Uncertainty quantification of the optimal stimulation area in an electro-stimulative hip revision system," in *Proc. IEEE 36th Int. Conf. Eng. Med. Biol. Soc.*, Aug. 2014, pp. 824–827.

[14] W. Paprosky and R. Magnus, "Principles of bonegrafting in revision total hip arthroplasty," *Clin. Orthop. Relat. Res.*, vol. 298, pp. 147–155, Jan. 1994.

[15] T. Weiland, "A discretization method for the solution of Maxwells equations for six-component fields," *Int. J. Electron. Commun.*, vol. 31, pp. 116–120, Feb. 1977.

[16] W. Kraus, "Magnetfeldtherapie und magnetisch induzierte Elektrostimulation in der Orthopädie," *Orthopädie*, vol. 13, pp. 78–92, Apr. 1984.

[17] K. Deb, A. Pratap, S. Agarwal, and T. Meyarivan, "A fast and elitist multiobjective genetic algorithm: NSGA-II," *IEEE Trans. Evol. Comput.*, vol. 6, no. 2, pp. 182–197, Apr. 2002.

[18] R. Byrd, R. Schnabel, and G. Shultz, "A trust region algorithm for nonlinearly constrained optimization," *SIAM J. Numer. Anal.*, vol. 24, pp. 1152–1170, Oct. 1987.

[19] G. Schmid, G. Neubauer, U. Illievich, and F. Alesch, "Dielectric Properties of porcine brain tissue in the transition from life to death at frequencies from 800 to 1900 MHz," *IEEE Trans. Evol. Comput.*, vol. 24, no. 6, pp. 413–422, Sep. 2003.

[20] D. Xiu, *Numerical Methods for Stochastic Computations: A Spectral Method Approach*. Princeton, NJ, USA: Princeton Univ. Press, 2010.

[21] F. Nobile, R. Tempone, and C. G. Webster, "A sparse grid stochastic collocation method for partial differential equations with random input data," *SIAM J. Numer. Anal.*, vol. 46, no. 5, pp. 2309–2345, May 2008.

[22] P. G. Constantine, M. S. Eldred, and E. T. Phipps, "Sparse pseudospectral approximation method," *Comput. Methods Appl. Mech. Eng.*, vols. 229–232, pp. 1–12, Jul. 2012.

[23] P. R. Supronowicz, P. M. Ajayan, K. R. Ullmann, B. P. Arulanandam, D. W. Metzger, and R. Bizios, "Novel current-conducting composite substrates for exposing osteoblasts to alternating current stimulation," *J. Biomed. Mater. Res.*, vol. 59, no. 3, pp. 499–506, Jul. 2002.

[24] R. A. Gittens, R. Olivares-Navarrete, R. Rettew, R. J. Butera, F. M. Alamgir, B. D. Boyan, and Z. Schwartz, "Electrical polarization of titanium surfaces for the enhancement of osteoblast differentiation," *Bioelectromagnetics*, vol. 34, no. 8, pp. 599–612, Jul. 2013.

[25] P. Grunert, A. Jonitz-Heincke, Y. Su, R. Souffrant, D. Hansmann, H. Ewald, A. Krüger, W. Mittelmeier, and R. Bader, "Establishment of a novel in vitro test setup for electric and magnetic stimulation of human osteoblasts," *Cell Biochem. Biophys.*, vol. 70, pp. 805–817, Nov. 2014.

Christian Schmidt (M'12) received the Ph.D. degree from the Faculty of Computer Science and Electrical Engineering, University of Rostock, Rostock, Germany.

He is currently a Postdoctoral Researcher in computational engineering for applications of neuroscience and electrostimulative implants at the University of Rostock. His research interests include stochastical methods for uncertainty quantification for several applications in the field of bioelectrical engineering.

Ulf Zimmermann received the Diploma degree (comparable to the Master's degree) in electrical engineering from the University of Rostock, Rostock, Germany, in 2010, where he is currently working toward the Ph.D. degree.

His research interests include computational modeling and simulation of electrically stimulating implants within biological tissues.

Ursula van Rienen (M'01) received the venia legendi in "electromagnetic field theory" and "scientific computing" from the Technische Universität Darmstadt, Darmstadt, Germany, in 1997.

Since 1997, she has been the Chair in "Electromagnetic Field Theory" at the University of Rostock, Rostock, Germany. Her research interests include computational electromagnetics with various applications, ranging from biomedical engineering to accelerator physics.